Am J Transl Res 2020;12(9):4998-5014
www.ajtr.org /ISSN:1943-8141/AJTR0102576

Original Article

Exosomes released by human umbilical cord mesenchymal stem cells protect against renal interstitial fibrosis through ROS-mediated P38MAPK/ERK signaling pathway

Bo Liu[1,2], Dong Hu[2], Yu Zhou[2], Yihang Yu[2], Lianju Shen[2], Chunlan Long[2], Denis Butnaru[3], Peter Timashev[3], Dawei He[1], Tao Lin[1], Tao Xu[4], Deying Zhang[1,2], Guanghui Wei[1,2]

[1]Department of Urology, Children's Hospital of Chongqing Medical University, Chongqing 400014, China; [2]Ministry of Education Key Laboratory of Child Development and Disorders, Chongqing Key Laboratory of Pediatrics, Chongqing International Science and Technology Cooperation Center for Child Development and Disorders, Chongqing 400014, China; [3]Institute for Regenerative Medicine, Sechenov University, 8-2 Trubetskaya St., Moscow 119991, Russia; [4]Department of Mechanical Engineering, Biomanufacturing Center, Tsinghua University, Beijing 100084, China

Received September 20, 2019; Accepted May 8, 2020; Epub September 15, 2020; Published September 30, 2020

Abstract: Mesenchymal stem cells (MSCs) and their conditioned medium attenuate renal fibrosis in an irreversible model of unilateral ureteral obstruction (UUO). However, the key components that play a role in the paracrine effects of MSCs and their mechanisms of action are not well understood. Therefore, in this study, we investigated whether exosomes released by human umbilical cord mesenchymal stem cells (hucMSC-Ex) would be able to attenuate renal fibrosis in an irreversible model of UUO and further explored potential mechanisms. In vivo, rats were divided into four groups: sham operation, sham operation transplanted with hucMSC-Ex, UUO, and UUO transplanted with hucMSC-Ex. hucMSC-Ex was administered via the left renal artery after total ligation of the left ureter. Rats were sacrificed after 14 days of obstruction. Renal function such as serum creatinine (Scr) or blood urea nitrogen (BUN) were monitored over the period. Histological changes, proliferation and apoptosis in tubular epithelial cells, and the levels of oxidative stress were measured. In vitro, NRK-52E cells were incubated with or without 5 ng/ml TGF-β1 and co-incubated with or without hucMSC-Ex for 48 h. Apoptosis and the levels of oxidative stress of NRK-52E cells were also measured. In the UUO group, the level of BUN and Scr, and the level of apoptosis and oxidative stress were all increased. In addition, the renal tubular injury and tubulointerstitial fibrosis were evident. However, all the above indices decreased significantly after treatment with hucMSC-Ex. *In vitro*, hucMSC-Ex significantly inhibited TGF-β1-induced apoptosis of NRK-52E cells by altering the production of ROS. Furthermore, it was observed that hucMSC-Ex inhibited apoptosis by inhibiting the activation of p38 mitogen-activated protein kinase (p38MAPK)/extracellular-signal-regulated kinase (ERK) 1/2 pathway. In conclusion, the results showed that hucMSC-Ex had positive effects towards UUO-induced renal fibrosis and apoptosis of renal tubular epithelial cells, and its mechanism of action was associated with inhibition of ROS-mediated p38MAPK/ERK signaling pathway. These data suggest the potential application of hucMSC-Ex in the treatment of chronic kidney disease, and also reveal the underlying mechanism of hucMSC-Ex action.

Keywords: Unilateral ureteral obstruction, oxidative stress, apoptosis, human umbilical cord mesenchymal stem cells, exosomes

Introduction

Renal interstitial fibrosis is a common pathological mechanism for the progression of chronic kidney disease (CKD) to end-stage renal disease. It is characterized by proliferation of interstitial fibroblasts and excessive extracellular matrix deposition in renal interstitium [1]. In the past few years, a large number of studies have been conducted to clarify the pathogenesis of renal interstitial fibrosis, and there has been increasing evidence that oxidative stress plays an important role in its progression [2]. After the kidney is damaged, it produces reac-

tive oxygen species (ROS) that exceed its scavenging capacity. Excessive ROS damages the antioxidant enzymes and causes cell damage through lipid peroxidation, DNA fragmentation, and protein damage. In addition, ROS can also promote the progression of renal interstitial fibrosis by regulating the infiltration of inflammatory monocytes and macrophages [3].

Previous studies have shown that mesenchymal stem cell (MSC) and their conditioned medium relieve kidney damage and improve kidney function after UUO [4], ischemic-reperfusion injury [5] and platinum-induced kidney injury [6], suggesting that MSCs can repair kidney tissue through paracrine effects. The important role of exosomes in paracrine secretion of MSCs has attracted the attention of researchers [7]. Exosomes are 40-100 nm microvesicles that are secreted into the extracellular environment after the intracellular vesicles fuse with the plasma membrane. Exosomes are composed of lipid bilayers, proteins, mRNA, and miRNAs. After binding to the cell membrane, the exosomes can transfer biologically active contents to target cells [8]. Interestingly, recent studies have shown that exosomes play a central role in the repair of damaged tissues by MSCs [9]. Exosomes derived from MSCs (MSC-Ex) have achieved satisfactory results in myocardial infarction injury [10] and cisplatin-induced ovarian granulosa cell apoptosis [11]. However, the effect of MSC-Ex on CKD has not been reported. Therefore, in this study, we investigated the antioxidant roles of exosomes derived from human umbilical cord mesenchymal stem cells (hucMSC-Ex) in CKD and explored the specific mechanisms by which they function.

Materials and methods

Ethics statement

The present study was approved by the ethics committee of the Chongqing Medical University (File No. 2018-023) and adhered to the tenets of the Declaration of Helsinki. Additionally, the written informed consent was obtained from all study participants.

Isolation and identification of hucMSC-Ex

The hucMSCs were isolated, expanded and identified as our previously described [4, 12]. Exosomes were extracted from the hucMSCs supernatant according to the following method. 80% confluent hucMSCs in passage 3 were washed with PBS and cultured in serum-free medium for an additional 48 hours. The conditioned medium was collected and centrifuged sequentially at 300×g for 10 minutes and then at 2000×g for 10 minutes. After the centrifugation, the supernatant was filtered using a 0.22-μm filter (Millipore, USA) to remove the remaining cells and cell debris. The supernatant was then transferred to an Ultra-Clear™ tube (Millipore, USA) and ultra-centrifuged at 100,000×g for 2 hours to deposit hucMSC-Ex. Afterwards, the supernatant was decanted. Pelleted hucMSC-Ex were resuspended in PBS, centrifuged at 4000×g until the volume in the upper compartment was reduced to approximately 200 μl. In order to further purification, the liquid containing hucMSC-Ex was laid on top of 30% sucrose/D_2O cushion in a sterile Ultra-Clear™ tube (Beckman Coulter, Kraemer Boulevard Brea, CA, USA) and centrifuged at 100,000×g for 120 minutes at 4°C (Beckman Coulter, Sorvall, Avanti J-26 XP, fixed angle rotor). hucMSC-Ex protein contents were determined using the BCA assay following the instructions (Beyotime Biotechnology, China). The morphology of the collected exosomes was observed by transmission electron microscopy (TEM). The tetraspan molecules CD9, CD63 and CD81 (Abcam, UK) were verified by western blotting. hucMSC-Ex were stored at -80°C for downstream experiments.

In vitro and in vivo experimental models

Rat proximal tubular epithelial cell line (NRK-52E) was purchased from China Center for Type Culture Collection (CCTCC). Cells were cultured in DMEM medium containing 10% fetal bovine serum (FBS; Gibco, Grand Island, USA) and 2% penicillin/streptomycin at 37°C with 5% CO_2. NRK-52E cells were cultured at a density of 1×10^5 per well in six-well culture plates. Near confluent NRK-52E cells were incubated with serum-free media for 24 h to arrest and synchronize the cell growth. After that, the media were changed to fresh serum-free media that contained recombinant human transforming growth factors-β1 (TGF-β1) (R&D, Minneapolis, MN, USA) (5 ng/ml) with or without hucMSC-Ex (100 μg). After 48 h, the cells were collected for protein detection.

Male Sprague Dawley rats, weighing 190-210 g, were purchased from the Chongqing Medical University. The rats were raised in standard cages in a room with constant temperature and humidity on a 12 hours light-dark cycle. UUO and sham surgery were performed as previously described. In brief, rats were anaesthetized with sodium pentobarbital (30 mg/kg, i.p.), in the UUO group, the left ureter was exposed and ligated with 4-0 silk thread, in the sham group, the left ureter was dissociated but not ligated. After the model was successfully established, hucMSC-Ex (200 μg of exosomes dissolved in PBS) was injected through the left renal artery. Rats were divided into four groups as follows (n = 8 for each group): sham group, sham operation treated with hucMSC-Ex (control group), UUO group, UUO treated with hucMSC-Ex (hucMSC-Ex group). Blood samples were collected at 0, 3, 7, 14 days post-surgery in order to measure biochemical analysis, including serum creatinine (Cr) and blood urea nitrogen (BUN). The rats were sacrificed at the 14th day after surgery. The left kidney was immediately removed and cut into two coronal sections. A portion of the kidney was preserved in 4% paraformaldehyde at room temperature, and the rest was stored in liquid nitrogen.

Mitochondrial transmembrane potential

NRK-52E cells in six-well culture plates were treated as mentioned above. After 48 h, the culture medium was removed and the cells were washed with PBS once, 1 ml cell culture medium with 1 ml JC-1 staining solution were added and the cells were incubated at 37°C for 20 min. After incubation, the supernatant was discarded and the cells were washed twice with JC-1 staining buffer (1×). When the mitochondrial membrane potential is high, JC-1 aggregates in the matrix of mitochondria to form a polymer that can produce red fluorescence. When the mitochondrial membrane potential is low, JC-1 cannot accumulate in the matrix of mitochondria, where JC-1 is a monomer and can produce green fluorescence. The relative ratio of red and green fluorescence is used to measure the proportion of mitochondrial depolarization.

Annexin V-FITC/PI double staining apoptosis detection

The Annexin V-FITC/PI apoptosis detection kit (KeyGEN BioTECH) was used to detect apoptotic cells according to the manufacture's protocol. Briefly, following treatment of NRK-52E cells as mentioned above, the adherent cells were washed once with PBS and the cells were dissociated with trypsin. The cell suspension was centrifuged at 1500 rpm for 5 minutes. After discarding the supernatant, the collected cells were washed twice with PBS. Then, 500 μl of binding buffer was added to suspend cells. After adding 5 μl of Annexin V-FITC and 10 μl of PI solution, the mixture was incubated at room temperature for 15 min. Apoptotic cells were detected by flow cytometry and quantified according to the percentage of apoptotic cells.

Histological examination

Paraffin-embedded kidney tissues were cut into 4 μm thick sections and then deparaffinized and rehydrated before hematoxylin eosin (HE), periodic acid-Schiff (PAS) and Masson trichrome staining. Ten visual fields were randomly selected in digital images from each section under high-power fields (magnification ×400). Tubular damage was scored by calculation of the percentage of tubules that displayed cell necrosis, loss of the brush border, cast formation, and tubular dilatation as follows: 0, 0 to 5%; 1, 5 to 10%; 2, 11 to 25%; 3, 26 to 45%; 4, 46 to 75%, and 5, >76%. Masson trichrome staining was used to assess the severity of renal interstitial fibrosis. Fibrotic areas were quantified in selected fields with the use of Image-Pro Plus image analysis software, version 6.0 (Media Cybernetics, Inc., Rockville, MD, USA). The severity of tubulointerstitial fibrosis was calculated as the ratio of the fibrotic area to the total selected field.

DCF assay for reactive oxygen species (ROS)

Levels of intracellular ROS were determined using a peroxide-sensitive fluorescent probe 2', 7'-dichlorofluorescein diacetates (DCFH-DA, Molecular Probes). After the cells were treated with measures above, DCFH-DA at a final concentration of 20 uM was added and the cells were incubated for 30 min in an incubator with 5% CO_2 at 37°C. Cells were washed three times with serum-free medium to remove DCFH-DA that did not enter the cells. Levels of intracellular ROS was detected by Microplate Reader (BioTek Inc, Winooski, VT). The raw data from each individual experiment were normalized to untreated cells.

The same method was used to determine the level of ROS in the kidney tissue. Briefly, the tissue homogenate was diluted with 1:20 to 5 mg tissue/mL with ice-cold Locke's buffer. The reaction mixture (1 ml) containing Locke's buffer (pH 7.4), 0.2 ml homogenate and 10 μl DCFH-DA (5 uM) was incubated at room temperature for 15 min to allow DCFH-DA to enter the membrane and was hydrolyzed by esterase. After further incubation for 30 min, the fluorescence intensity was measured using a spectrophotometer, and the ROS production was quantified by a DCF standard curve. Data were expressed as pmol DCF formed/min/mg protein.

Measurement GSH or MDA in tissue or cells

Cell suspensions or kidney tissue were collected for detection of malondialdehyde (MDA) and glutathione (GSH). GSH and MDA assay kits were purchased from Jiancheng Bioengineering Institute (Nanjing, China). Briefly, *in vivo,* appropriate amount of kidney tissue was rinsed in cold saline to remove the residual blood, drawn moisture with filter paper and weighed. The homogenate medium (0.86% saline) was added at a pre-setting ratio (weight (g)/volume (ml) = 1:9). After full grinded, 10% tissue homogenate was centrifuged at 3000 rpm for 10 minutes. *In vitro,* the cells were collected and purified by sonication. The BCA assay kit (Beyotime, China) was used to determine the protein concentration in tissues or cells. MDA and GSH were measured according to the instructions.

Terminal-deoxynucleoitidyl transferase mediated nick end labeling (TUNEL) assay

Tissue slices were dewaxed and hydrated, and the number of apoptotic cells in the renal tubular epithelium was measured by the TUNEL assay using an *in situ* cell death detection kit (Roche, Indianapolis, IN, USA) according to the manufacturer's instructions.

Immunofluorescent and immunohistochemistry

NRE-52E cells were treated as described above, fixed with 4% paraformaldehyde, and permeabilized with Triton X100 (Solarbio, China). The cells slides were then blocked with 5% BSA (BD, USA) and incubated with rabbit anti-phosphorylated p38 (1:200; CST, USA) or rabbit anti-phosphorylated Erk1/2 (1:200; CST, USA) at 4°C overnight. After washing three times with PBS, the corresponding fluorescent secondary antibody (ZSGB-BIO, China) was added to incubate for 1 hour. The nuclei were then counterstained with DAPI (Beyotime, China) and the images were examined under a fluorescence microscope (K10587; Nikon, Japan).

The kidney tissue slices underwent dewaxing and hydration, antigen was retrieved by citric acid buffer (PH 6.0) microwave antigen retrieval. After natural cooling, the endogenous peroxidase was blocked with 3% H_2O_2 for 10 min, then the non-specific protein binding site was blocked with 0.5% BSA for 1 hour. slices were incubated at 4°C with 1:200 diluted rabbit anti-phosphorylated p38 (CST), rabbit anti-phosphorylated Erk1/2 (CST), and mouse anti-PCNA (Abcam), respectively. Slices were washed three times with PBS, then with the goat anti-rabbit or anti-mouse antibody (Zhongshan, Beijing, China) at 37°C for 1 hour. After sections were counterstained with haematoxylin, positive staining was developed by incubation with 3, 3'-diamnobenzidine (DAB). The number of PCNA-positive cells and the intensity of cleaved-caspase 3, Bax, Bcl-2 were assessed under five randomly selected high power field (×400). Image Pro Plus 6.0 was used as a tool to quantify the integrated optical density (IOD) of positive areas.

Western blot analysis

Kidney tissues and cells were lysed in RIPA Lysis Buffer (Beyotime, China) containing phenylmethylsulfonyl fluoride (PMSF), and centrifuged at 4°C at 12,000 rpm for 20 min. The protein concentration was measured using the BCA assay kit (Beyotime, China). SDS-PAGE (Sodium dodecyl sulfate polyacrylamide gel electrophoresis) loading buffer was mixed with protein samples and boiled last for 10 min. The proteins were electrophoresed through SDS-polyacrylamide gels. After that, proteins were transferred to PVDF (Polyvinylidene fluoride) membranes (Millipore, USA). In order to block nonspecific protein background, membranes were blocked in 5% skim milk for 1 hour with shaker. After that, the protein bands were incubated overnight at 4°C with the following primary antibodies: rabbit anti-CD9 (1:2000; Abcam, USA), rabbit anti-CD63 (1:1000; Abcam, USA), rabbit anti-CD81 (1:1000; Abcam, USA), rabbit anti-p38MAPK (1:1000; CST, USA),

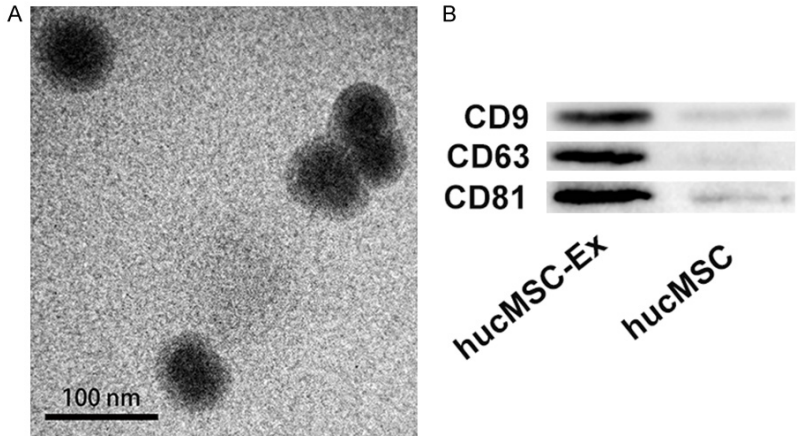

Figure 1. Characterization of exosomes derived from human umbilical cord mesenchymal stem cells (hucMSC-Ex). A. Electron microscopy analysis of exosomes secreted by hucMSCs (scale bar = 100 nm). B. Exsome-specific markers CD9, CD63 and CD81 were measured by western blot analysis. Ex exosome; hucMSC human umbilical cord-derived mesenchymal stem cell.

rabbit anti-phosphorylated-p38MAPK (1:1000; CST, USA), rabbit anti-ERK1/2 (1:1000; CST, USA), rabbit anti-phosphorylated-ERK1/2 (1:1000; CST, USA), Mouse anti-PCNA (1:1000; Abcam, USA), rabbit anti-Cleaved caspase-3 (1:1000; Abcam, USA), rabbit anti-Bax (1:1000; Abcam, USA), mouse anti-Bcl-2 antibody (1:1000; Abcam, USA), β-actin (Zhongshan, China). The membrane was then washed three times with Tris-buffered saline/Tween (TBST) and incubated in goat anti-rabbit or mouse antibodies (1:500; Zhongshan, China) for 2 hours at 37°C. Immobilon Western Chemiluminescent HRP Substrate (Millipore, USA) were used to detect positive immune reactions.

Statistical analysis

The data obtained from the experiment were expressed as mean ± standard deviation (mean ± SD). The mean value of each group was compared with one-way analysis of variance (ANOVA) followed by a Dunnett's post hoc test. When the *P* value is less than 0.05, the difference was considered to be statistically significant. All data were analyzed by SPSS 16.0 software.

Results

The characterization of hucMSCs and hucMSC-Ex

Flow cytometry analysis showed that hucMSCs had typical surface markers of mesenchymal stem cells, high expression of CD73, CD90, CD105, but negative expression of CD34, CD45, and HLA-DR. HucMSCs were induced by adipogenic and osteogenic medium. After adipogenic induction, the cells were stained with oil red O, and red lipid droplets were observed in the cytoplas. After osteogenesis induction, the cells were stained with alizarin red, and red mineralized nodules are visible in cell culture dishes. These results suggesting that hucMSCs has the ability to differentiate into adipocytes and osteocytes [12].

The morphology of hucMSC-Ex was observed under transmission electron microscope, and it was seen that the exosomes were round or oval and had a diameter of about 50-100 nm (**Figure 1A**). Western blot analysis showed that hucMSC-Ex expressed exosomes biomarkers such as CD9, CD63, and CD81 (**Figure 1B**).

HucMSC-Ex inhibited morphologic changes of NRK-52E cells induced by TGF-β1

In vitro, we used TGF-β1 to induce NRK-52E cells to mimic the renal tubular epithelial cells morphologic changes in CKD and to verify the effect of hucMSC-Ex on it. After cultured with serum-free medium for 12 h, NRK-52E cells were treated with TGF-β1 for another 48 h with or without hucMSC-Ex. The morphological features of cell growth were observed under inverted microscope. Normal NRK-52E cells were round or oval, and displayed typical cobblestone-like morphology. After TGF-β1 induction, the cells became long spindle-shaped, and the intercellular junction reduced. However, hucMSCs-Ex significantly inhibited TGF-β1-induced NRK-52E cells morphologic changes (**Figure 2A**).

Effects of in vitro co-culturing of TGF-β1-induced NRK-52E cells with hucMSC-Ex on the mitochondrial membrane potential

NRK-52E was stained with JC-1 dye and observed under fluorescence microscope. As shown in **Figure 2B**, the red fluorescence indicates that JC-1 aggregates the polymer in the

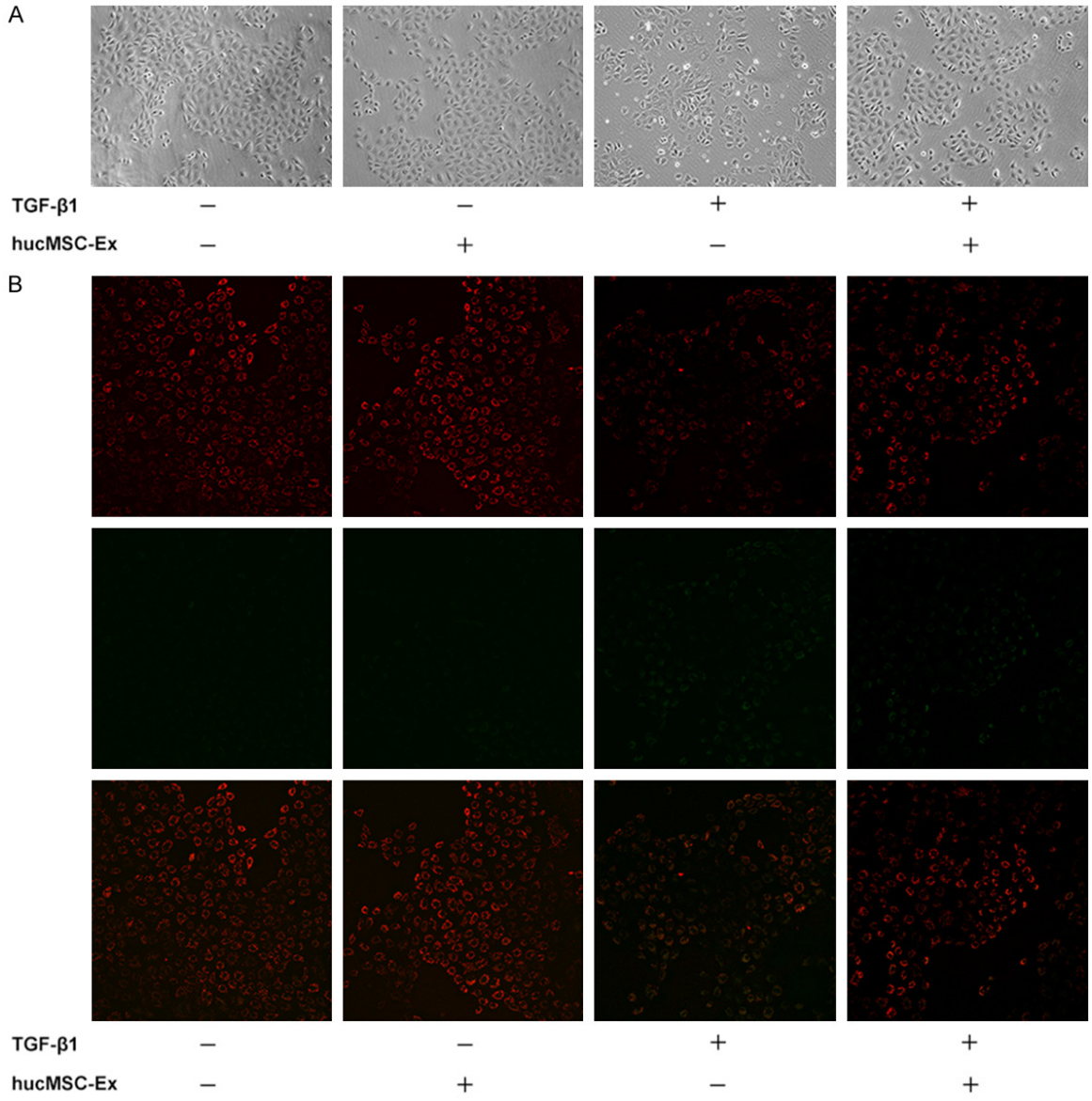

Figure 2. The effect of hucMSC-Ex on the morphology and mitochondrial membrane of TGF-β1-induced NRK-52E cells. A. The effects of hucMSC-Ex on cell morphology transformation. NRK-52E cells changed from a cuboidal to a spindle shape in response to TGF-β1, whereas treatment with hucMSC-Ex blocked this morphological transformation. B. Effect of co-culture of TGF-β1-induced NRK-52E cells on the mitochondrial membrane potential (ΔΨm). The ΔΨm detected by JC-1 fluorescent probe. Red florescence indicates that JC-1 aggregates formed in cells with a high ΔΨm, whereas green fluorescence indicates that JC-1 monomers formed in cells with low ΔΨm. Ex exosome, hucMSC human umbilical cord-derived mesenchymal stem cell, TGF-β1 transforming growth factor β1.

normal NRK-52E cell mitochondria with high membrane potential, whereas the green fluorescence indicates that JC-1 cannot accumulate in the TGF-β1-induced cell mitochondria with low membrane potential, thus forming a monomer. The increase of the ratio of green fluorescence to red fluorescence represents the decrease of mitochondrial membrane potential, suggesting that TGF-β1 induced early apoptosis of NRK-52E cells. After hucMSC-Ex treatment, the ratio of green fluorescence to red fluorescence decreased, which indicated that the apoptosis rate of NRK-52E cells decreased.

HucMSC-Ex inhibited the production of ROS and oxidative stress in NRK-52E cells induced by TGF-β1

Many research findings revealed that oxidative stress may induce apoptosis [13]. To assess the protective effect of hucMSC-Ex on TGF-β1-

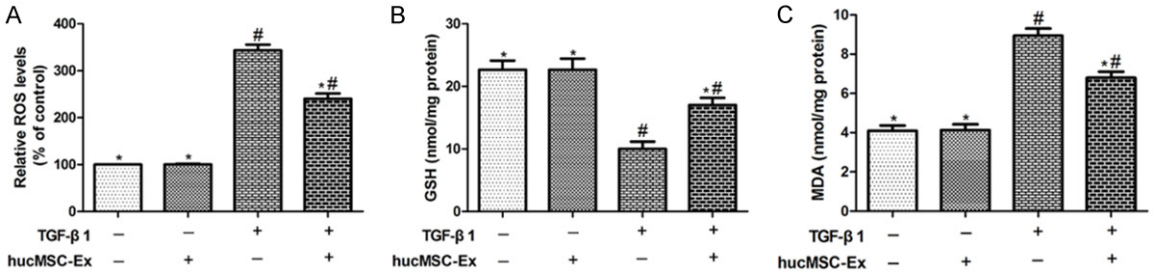

Figure 3. The effect of hucMSC-Ex on oxidative stress levels in TGF-β1-induced NRK-52E cells. A. The levels of ROS in each group. B. The levels of GSH in each group. C. The levels of MDA in each group. Values presented as mean ± SD. $^{*}P<0.05$ versus TGF-β1 alone treated group; $^{\#}P<0.05$ versus control group. Ex exosome, GSH glutathione, hucMSC human umbilical cord-derived mesenchymal stem cell, MDA malondialdehyde, ROS reactive oxygen species, TGF-β1 transforming growth factor β1.

induced apoptosis, we used semi-quantitative flow cytometry to estimate intracellular ROS levels based on DCF fluorescence intensity. Our results show that TGF-β1 induces ROS overproduction in NRK-52E cells. However, hucMSC-Ex inhibits oxidative stress by reducing ROS production. At the same time, we tested the level of oxidative stress in each group of NRK-52E cells. Compared with the control group, the level of GSH in TGF-β1 group decreased, and the level of MDA increased. However, the level of GSH in hucMSC-Ex group was significantly higher than that in TGF-β1 group, and the level of MDA was significantly decreased, suggesting that antioxidant stress effects of hucMSC-Ex plays an important role in the inhibition of NRK-52E cells apoptosis (**Figure 3**).

HucMSC-Ex suppressed TGF-β1-induced apoptosis and promoted proliferation in NRK-52E cells

In order to further study the role of hucMSC-Ex in inhibiting TGF-β1-induced apoptosis of NRK-52E cells, hucMSC-Ex were co-cultured with TGF-β1 in the NRK-52E cells for 48 h. Flow cytometry analysis showed that the apoptosis rate of NRK-52E cells induced by TGF-β1 was 10.4%, but the apoptosis rate was reduced to 8.3% after application of hucMSC-Ex (**Figure 4A**, **4B**). Western blot analysis was used to detect the expression of PCNA, cleaved caspase-3, bax and bcl-2. After TGF-β1 induced NRK-52E cells apoptosis, the activation level of cleaved caspase-3 and Bax were significantly increased, while the level of apoptotic protein Bcl-2 decreased. After treatment of hucMSC-Ex, the levels of cleaved-caspase 3 and Bax decreased, and the level of Bcl-2 increased. Western blot also showed a decrease in the expression level of PCNA after TGF-β1 induced apoptosis, but the expression of PCNA increased after treatment of hucMSC-Ex (**Figure 4C-G**).

Next, we detected the activation level of P38MAPK/ERK signaling pathway in each group. Immunofluorescence staining and western blot showed that TGF-β1 could activate P38MAPK/ERK signal pathway in NRK-52E cells, which showed that the expression levels of p-P38, p-ERK increased, while hucMSC-Ex inhibited P38MAPK/ERK signaling pathway activation (**Figure 5**).

HucMSC-Ex improved renal histomorphology and renal function in rats with CKD

In order to assess the renal histomorphology of each group, paraffin specimens were cut to 4 μm thickness and stained with HE, PAS and Masson's trichrome. There were no obvious histological abnormalities in the sham group and the control group. At 14 days after operation, the UUO group showed tubular dilation or atrophy, vascular collapse, inflammatory cell infiltration, extracellular matrix deposition, and significant interstitial fibrosis. However, the number and extent of renal tubular injury in hucMSC-Ex group were significantly lower than those in UUO group. The area of renal interstitial fibrosis in UUO group was significantly higher than that in sham group and control group at 14 days after operation. Further, the interstitial fibrosis area of hucMSC-Ex group was significantly lower than that of UUO group (**Figure 6A-C**). Therefore, hucMSC-Ex can improve the progression of renal interstitial fibrosis caused by UUO in CKD.

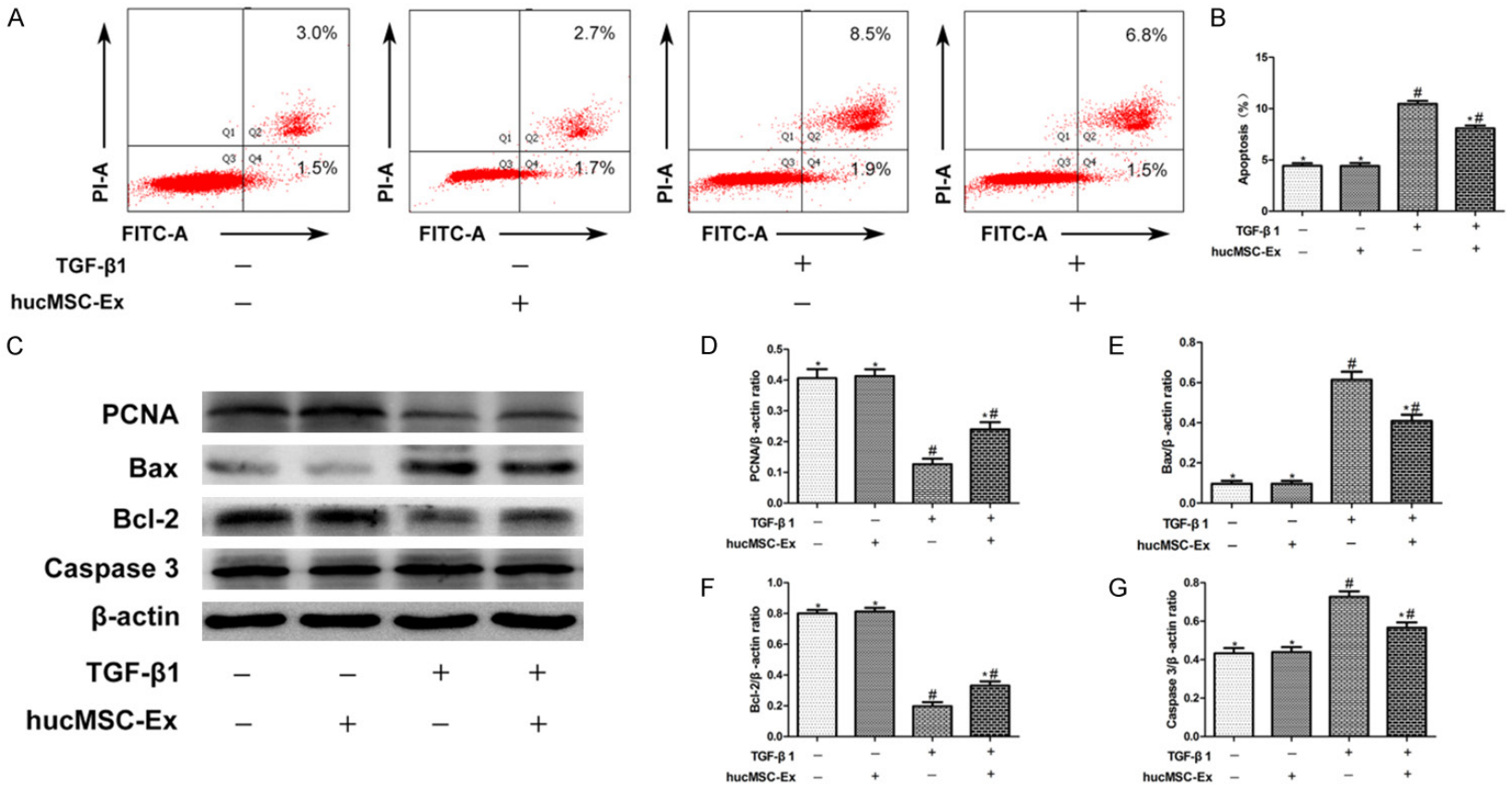

Figure 4. The effect of hucMSC-Ex on proliferation and apoptosis in TGF-β1-induced NRK-52E cells. A. Cells were double-stained with Annexin V-FITC and PI and were then analysed using flow cytometry. B. Statistical analysis of the proportions of early apoptosis and later apoptosis of NRK-52E cells. C. Western blot analysis of PCNA, Bax, Bcl-2, and Cleaved caspase-3 protein in each group. D-G. Relative protein expression levels in each group. β-actin used as inner reference and quantified using densitometric analysis. Values presented as mean ± SD. $^{*}P<0.05$ versus TGF-β1 alone treated group; $^{\#}P<0.05$ versus control group. Bax B-cell lymphoma/leukemia-2 associated X protein, Bcl-2 B-cell lymphoma/leukemia-2, Ex exosome, hucMSC human umbilical cord-derived mesenchymal stem cell, PCNA proliferating cell nuclear antigen, TGF-β1 transforming growth factor β1.

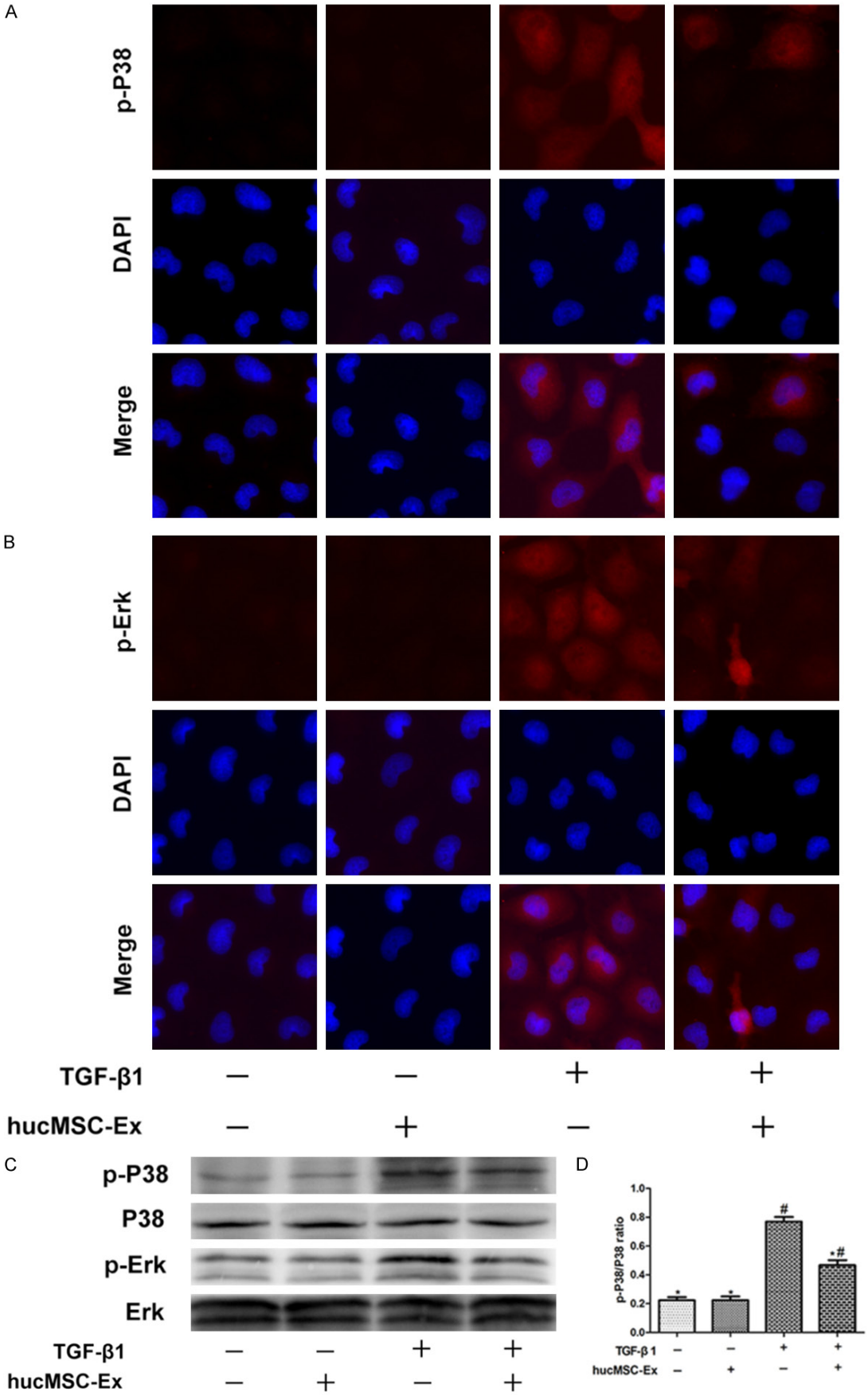
A
p-P38
DAPI
Merge
B
p-Erk
DAPI
Merge
TGF-β1 — — + +
hucMSC-Ex — + — +
C
p-P38
P38
p-Erk
Erk
TGF-β1 — — + +
hucMSC-Ex — + — +
D
p-P38/P38 ratio
1.0
0.8
0.6
0.4
0.2
0.0
#
*#
*
*
TGF-β1 – – + +
hucMSC-Ex – + – +

Figure 5. The effect of hucMSC-Ex on expression of p38MAPK, Erk1/2 in TGF-β1-induced NRK-52E cells. A, B. Immunofluorescent staining of p-P38 and p-Erk in each group. C. Western blot analysis of p-P38, P38, p-Erk, and Erk protein in each group. D, E. Relative protein expression levels in each group. P38MAPK and Erk1/2 used as inner reference and quantified using densitometric analysis. Values presented as mean ± SD. $^{*}P<0.05$ versus TGF-β1 alone treated group; $^{\#}P<0.05$ versus control group. Erk1/2 Extracellular regulated kinase 1/2, Ex exosome, hucMSC human umbilical cord-derived mesenchymal stem cell, P38MAPK mitogen-activated protein kinase P38, TGF-β1 transforming growth factor β1.

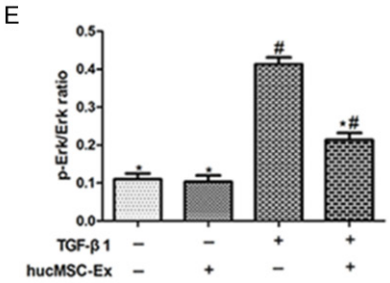

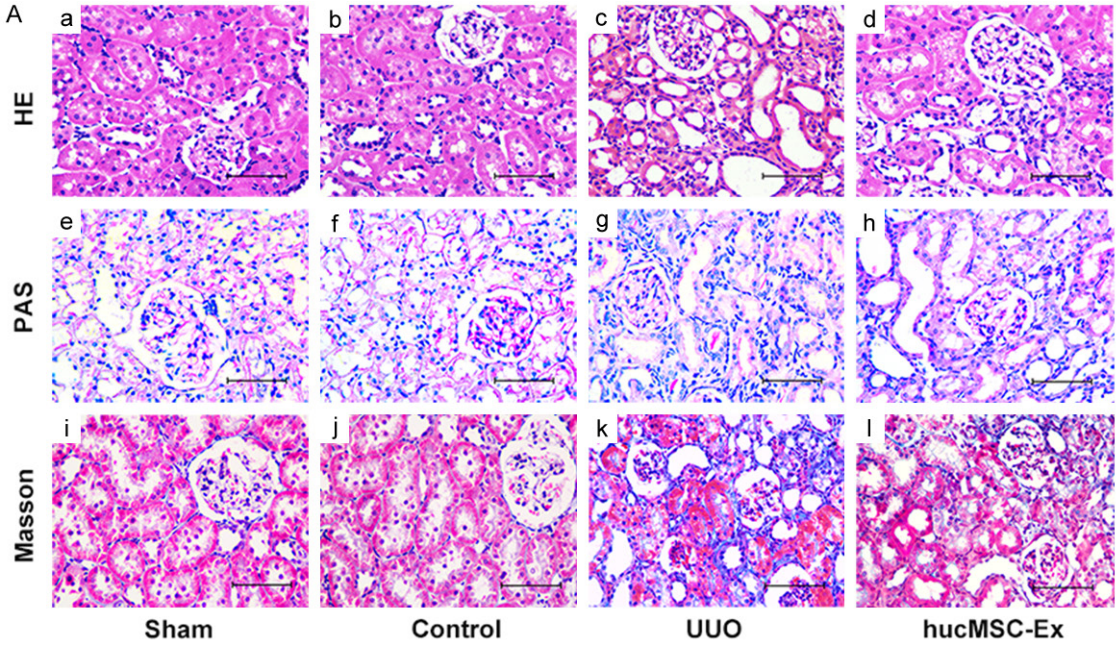

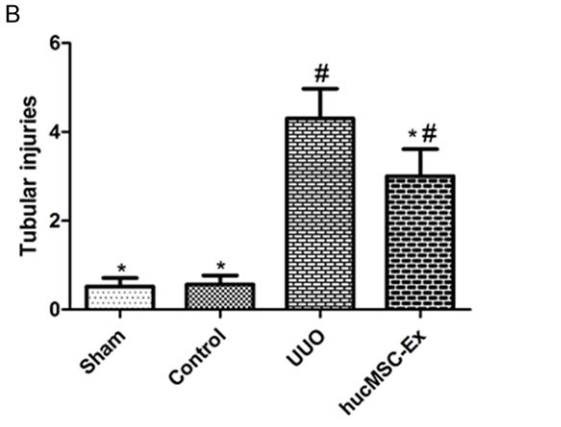

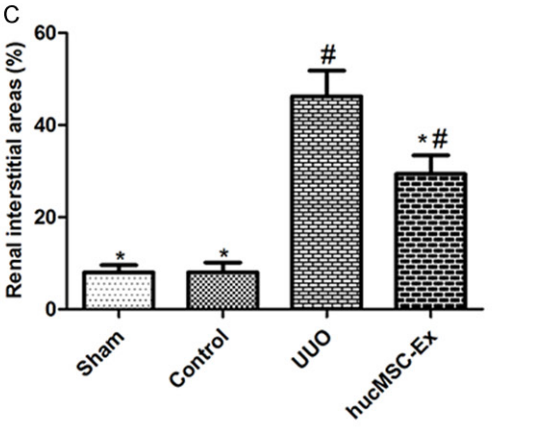

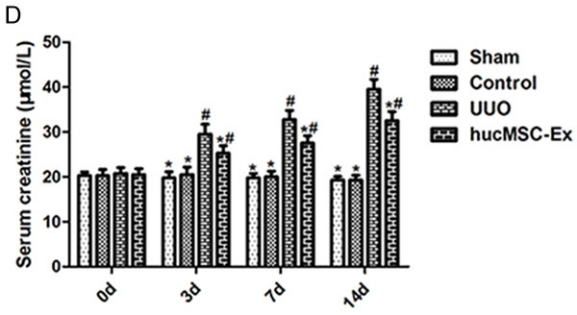

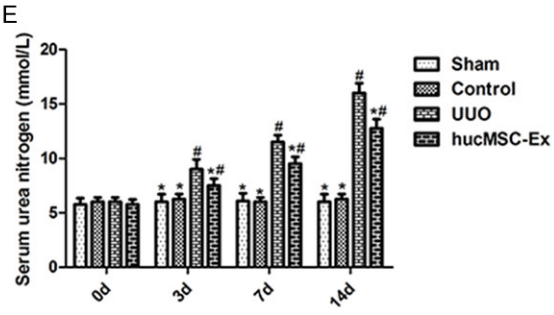

Figure 6. The effect of hucMSC-Ex on the histopathology and function of UUO-induced kidneys. (A) Histopathology analysis of the kidney in each group. (a-d) H&E staining, (e-h) PAS staining, (i-l) Masson's trichrome staining. (B) Tubular damage was scored by calculation of the percentage of tubules that displayed cell necrosis, loss of the brush border, cast formation, and tubular dilatation. (C) Area of renal interstitial fibrosis in each group. (D, E) BUN and Scr values in each group at 0, 3, 7, 14 days. Values presented as mean ± SD. $^{*}P<0.05$ versus UUO group; $^{\#}P<0.05$ versus sham and control group. BUN blood urea nitrogen, Ex exosome, HE hematoxylin-eosin, hucMSC human umbilical cord-derived mesenchymal stem cell, PAS periodic acid schiff, Scr serum creatinine, UUO unilateral ureteral obstruction.

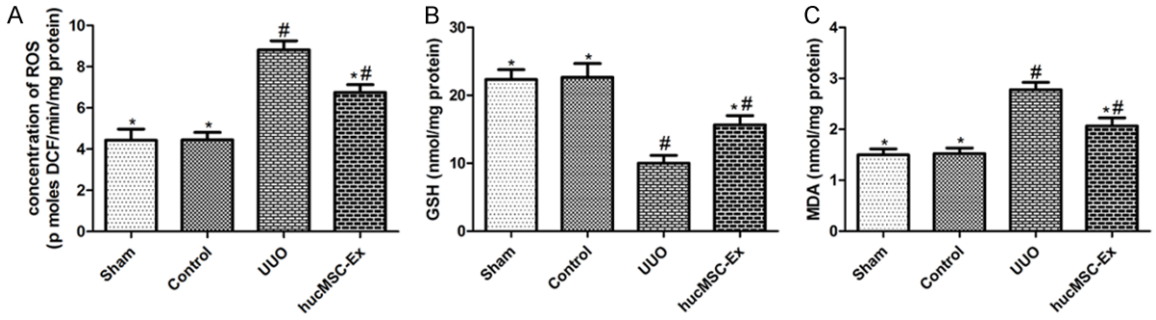

Figure 7. The effect of hucMSC-Ex on oxidative stress levels in UUO-induced kidneys. A. The levels of ROS in each group. B. The levels of GSH in each group. C. The levels of MDA in each group. Values presented as mean ± SD. $^{*}P<0.05$ versus UUO group; $^{\#}P<0.05$ versus sham and control group. Ex exosome, GSH glutathione, hucMSC human umbilical cord-derived mesenchymal stem cell, MDA malondialdehyde, ROS reactive oxygen species, UUO unilateral ureteral obstruction.

To further assess the number and extent of renal tubular damage, we stained paraffin sections with PAS. Sham group and control group showed renal tubular and glomerular structure integrity. 14 days after surgery, the UUO group had atrophy or dilation of the renal tubules, and the protein cast was formed in the proximal tubule and the distal tubule. At the same time, the brush border was destructed and renal fibrosis was significant. However, the renal tubular injury was reduced in hucMSC-Ex group compared to UUO group (**Figure 6A-C**). Therefore, hucMSC-Ex transplantation can reduce renal tubular injury in rats with CKD. Consistent with the above histological changes, serum creatinine and urea nitrogen were significantly increased after UUO. However, compared with UUO group, the levels of serum creatinine and urea nitrogen in hucMSC-Ex group were decreased at 3 d, 7 d and 14 d after operation, suggesting that hucMSC-Ex could effectively delay the deterioration of renal function in CKD rats (**Figure 6D**, **6E**).

HucMSC-Ex inhibited the production of ROS and oxidative stress in UUO-induced kidney

ROS plays an important role in UUO-induced renal injury, which is an oxidative product of free radicals acting on lipid peroxidation [14]. Some studies have shown that MDA in obstructive renal tissue is higher than normal renal tissue [15]. Our study also found that the levels of MDA and ROS in the UUO group were higher than those in the sham and control groups, but hucMSC-Ex could significantly prevent the increase of MDA and ROS level in UUO-induced kidney. Compared with sham and control group, the level of GSH in UUO group was significantly decreased, but the level of GSH in hucMSC-Ex group was significantly higher than that in UUO group (**Figure 7**).

HucMSC-Ex suppressed UUO-induced apoptosis and promoted proliferation in rats

As shown in **Figure 8A-D**, there were few PCNA-positive cells and Tunel-positive cells in the sham and control group. Compared with the UUO group, the number of PCNA-positive cells was significantly increased in the hucMSC-Ex group, while the number of Tunel-positive cells was significantly reduced. The expression of Bax, Bcl-2 and cleaved caspase-3 in renal tissue were detected by western blotting. Compared with sham group and control group, the levels of Bax and cleaved caspase-3 in UUO group were significantly increased, and their expression was decreased after hucMSC-Ex treatment. The levels of Bcl-2 was also altered, and the level of Bcl-2 in UUO-induced kidney were significantly increased after hucMSC-Ex treatment (**Figure 8E-H**).

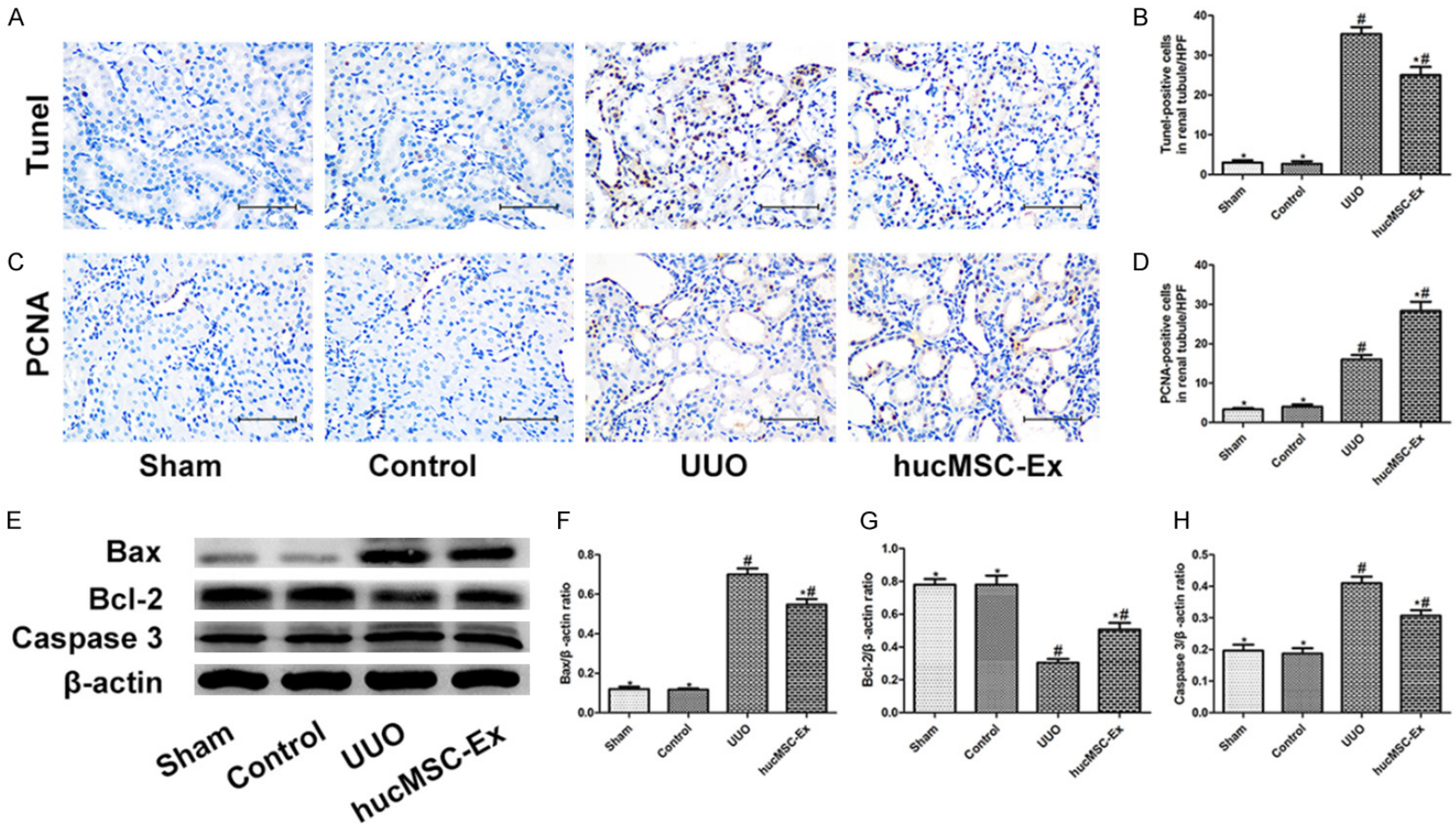

Figure 8. The effect of hucMSC-Ex on proliferation and apoptosis in UUO-induced kidneys. A, B. Tunel-positive cells of renal tubules in each group. C, D. PCNA-positive cells of renal tubules in each group. E. Western blot analysis of Bax, Bcl-2, and Cleaved caspase-3 protein in each group. F-H. Relative protein expression levels in each group. β-actin used as inner reference and quantified using densitometric analysis. Values presented as mean ± SD. $^{*}P<0.05$ versus UUO group; $^{\#}P<0.05$ versus sham and control group. Bax B-cell lymphoma/leukemia-2 associated X protein, Bcl-2 B-cell lymphoma/leukemia-2, Ex exosome, hucMSC human umbilical cord-derived mesenchymal stem cell, PCNA proliferating cell nuclear antigen, Tunel terminal-deoxynucleoitidyl transferase mediated nick end labeling, UUO unilateral ureteral obstruction.

Similarly, we detected the activation of P38-MAPK/ERK signaling pathway in kidney tissue by immunohistochemical staining and western blotting. The results showed that p-p38 and p-ERK were significantly increased in UUO-induced kidney, and the activation of P38-MAPK/ERK signaling pathway was significantly inhibited by hucMSC-Ex treatment (**Figure 9**).

Discussion

In recent years, MSC have been shown to have a good prospect in the treatment of autoimmune diseases, myocardial infarction, spinal cord injury and other refractory diseases [16]. MSC transplantation has become a new treatment of nephropathy and has entered clinical trials [17]. However, the exact mechanism of MSC repairing kidney injury is unclear. MSCs are currently known to have multiple differentiation potentials. Nevertheless, more and more studies have shown that secreted active substances of MSC play an important role in kidney injury repair [4, 12]. Recent studies also suggest that exosomes secreted by MSC may be a new way to deliver repair information [18, 19].

Exosomes is a homogeneous membrane vesicle with a diameter of 40-100 nm secreted by cells in physiological or pathological conditions [20]. MSC-Ex contains a large number and a wide variety of protein, mRNA and miRNA and other bioactive substances. MSC-Ex translates the biologically active substance into the target cells by membrane fusion or endocytosis, thereby affecting the function of the target cells. MSC-Ex can mediate cell-to-cell information delivery while also simulating the biological functions of the MSC, such as promoting tissue repair and immunoregulation [21]. Our results show that hucMSC-Ex expresses exosomes surface markers such as CD9, CD63 and CD81, and hucMSC-Ex is spherical and has a diameter of about 40-100 nm under transmission electron microscopy.

Recent studies [22, 23] have shown that UUO-induced renal damage is associated with oxidative stress-induced renal tubular epithelial apoptosis, so our aim is to investigate whether hucMSC-Ex can reduce UUO-induced oxidative stress injury and reduce renal tubular epithelial apoptosis. *In vivo*, we found that hucMSC-Ex can repair UUO-damaged renal tubules, reduce renal tubular damage and renal interstitial fibrosis, thereby reducing the levels of serum creatinine and urea nitrogen. *In vitro*, we first detected the mitochondrial membrane potential changes to determine the early apoptosis of cells. Endogenous or exogenous damage signals can induce mitochondrial membrane permeability changes, causing mitochondrial transmembrane potential decreased, leading to the apoptosis-related gene expression, and ultimately lead to cell apoptosis [24]. JC-1 from the red fluorescence to green fluorescence means that the mitochondrial membrane potential decline, representing the cells are in the early phase of apoptosis. After treatment with TGF-β1, the ratio of green to red fluorescence of NRK-52E cells was increased, and the ratio decreased after hucMSC-Ex treatment. We also observed an increase in apoptosis of renal tubular epithelial cells after TGF-β1 treatment, and a significant reduction in apoptotic cells after hucMSC-Ex treatment. In addition, the expression of pro-apoptotic protein Bax increased, and anti-apoptotic protein Bcl-2 decreased after UUO. After Treatment with hucMSC-Ex, the expression of Bax protein was significantly decreased, and the expression of Bcl-2 protein was significantly increased. In the *in vitro* experiment, we observed the same phenomenon.

Kidney tissue requires higher oxygen consumption to complete the active transport and reabsorption of water and electrolytes, so the tubules are susceptible to oxidative stress injury [25]. Studies have shown that renal ischemia-reperfusion injury [26] and cisplatin cytotoxicity [27] can cause increased oxidative stress. At present, the pathological damage of renal injury is mainly associated with ischemia, hypoxia, and reactive oxygen species [28]. Lipid peroxidation refers to the process of oxidation of unsaturated fatty acids under the attack of oxygen free radicals, resulting in a series of reactive oxygen species. Lipid peroxidation can damage the integrity of the membrane, causing cell inflammation [29]. Our study found that after hucMSC-Ex treatment, the ROS of UUO kidney decreased significantly, suggesting that hucMSC-Ex has a certain antioxidant effect. MDA is a product of lipid peroxidation, which can destroy the structure and function of the cell membrane, also is toxic to cells and can stimulate the expression of collagen gene in interstitial cells. Changes in amount of MDA

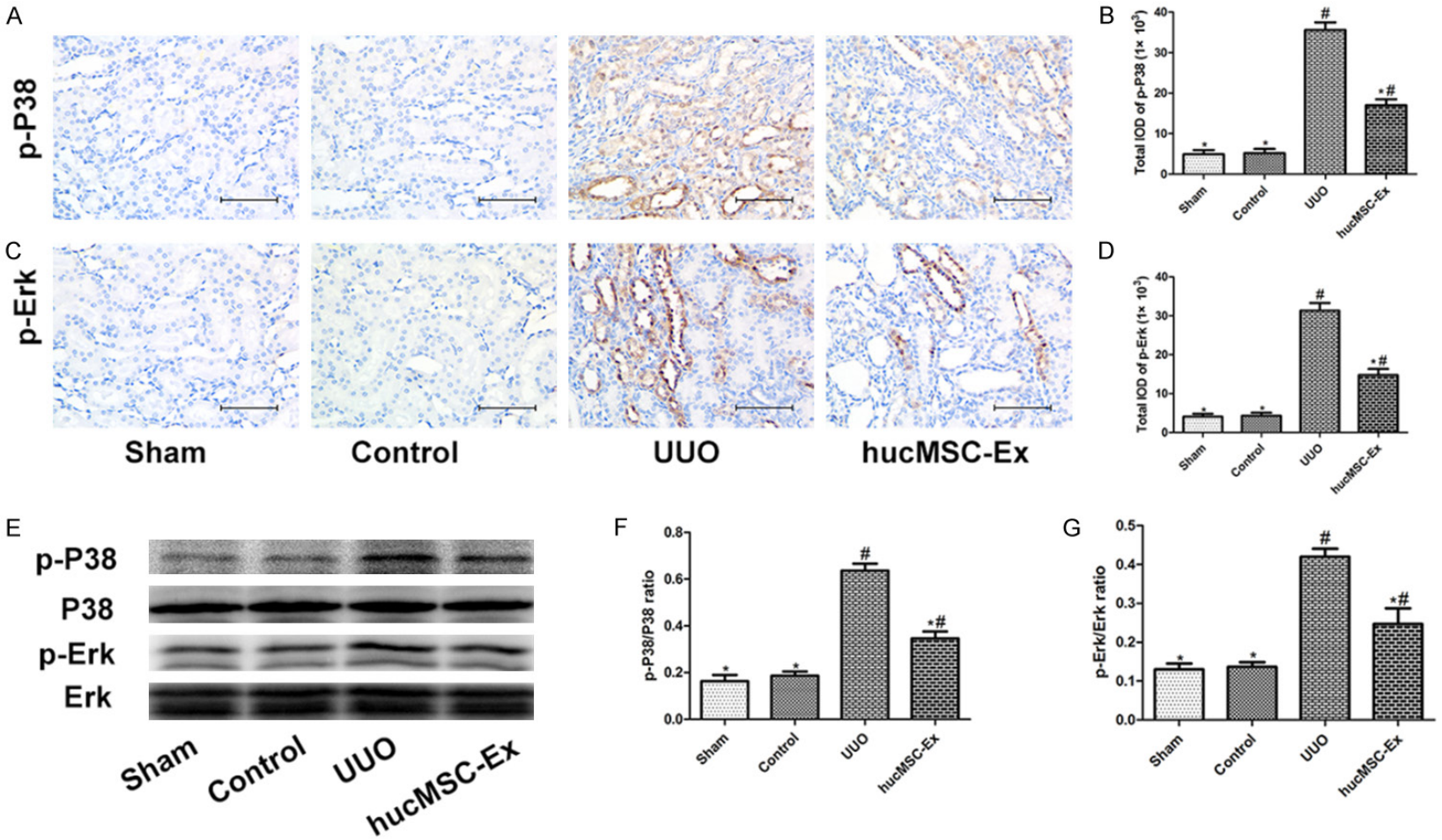

Figure 9. The effect of hucMSC-Ex on expression of P38MAPK, Erk1/2 in UUO-induced kidneys. A. Immunohistochemical staining of p-P38 in each group. B. Total IOD of p-P38 in each group. C. Immunohistochemical staining of p-Erk in each group. D. Total IOD of p-Erk in each group. E. Western blot analysis of p-P38, P38, p-Erk, and Erk protein in each group. F, G. Relative protein expression levels in each group. P38MAPK and Erk1/2 used as inner reference and quantified using densitometric analysis. Values presented as mean ± SD. $^{*}P<0.05$ versus UUO group; $^{\#}P<0.05$ versus sham and control group. Erk1/2 Extracellular regulated kinase 1/2, Ex exosome, hucMSC human umbilical cord-derived mesenchymal stem cell, IOD integrated optical density, P38MAPK mitogen-activated protein kinase P38, UUO unilateral ureteral obstruction.

represent the level of lipid peroxidation, indirectly reflecting the extent of cell damage [30]. GSH is an important antioxidant and free radical scavenger, which plays an important role in maintaining the biological function of cells and protecting the integrity of cell membrane [31]. The level of MDA in NRK-52E cells induced by TGF-β1 and UUO kidney was significantly increased, while the level of GSH was significantly decreased. Thus, hucMSC-Ex treatment can reduce the level of MDA, while increasing the level of GSH.

We observed that hucMSC-Ex not only inhibit the apoptosis of renal tubular epithelial cells, but also promote the proliferation of renal tubular epithelial cells, showing the number of PCNA positive cells and protein expression increased. However, the specific mechanism is still unclear. Mitogen-activated protein kinase (MAPK) signal transduction pathway is a class of important signaling systems in which eukaryotic cells transduce extracellular signals into the cell and cause cellular biological responses [32]. Accumulating evidence suggests that members of the MAPK family play an important role in ROS-mediated apoptosis [33]. In the three known MAPK signaling pathways, ERK-associated intracellular signal transduction pathways are considered to be classical MAPK signal transduction pathways. It is known that P38MAPK and ERK1/2 signal transduction pathway regulates cell growth and differentiation, but growing evidence suggests that activation of P38MAPK and ERK1/2 also plays a role in cell death [34]. Our results suggest that the P38MAPK/ERK signaling pathway is activated in TGF-β1-induced NRK-52E cells or UUO kidney, thereby initiating apoptosis and promoting the expression of apoptotic protein cleaved caspase-3, whereas hucMSC-Ex inhibits P38MAPK/ERK signaling pathway, thereby inhibiting the expression of cleaved caspase-3.

Conclusions

Current study has shown that a concurrent activation of P38MAPK/ERK pathway is involved in UUO-induced renal injuries and that hucMSC-Ex protects UUO kidney against oxidative stress injuries via inhibition of ROS-activated P38MAPK/ERK pathway. Continued attempts to clarify that the target molecules after P38MAPK and ERK1/2 pathway activation and the crosstalk of the upstream and downstream signaling molecules will help to further clarify the cellular and molecular mechanisms for the protective effect of hucMSC-Ex on chronic kidney disease.

Acknowledgements

This work was supported by National Natural Science Foundation of China Grant 81800618.

Disclosure of conflict of interest

None.

Address correspondence to: Drs. Deying Zhang and Guanghui Wei, Department of Urology, Children's Hospital of Chongqing Medical University, No. 136, Zhongshan 2 RD, Yuzhong District, Chongqing 400014, China. Tel: +86-13594136249; E-mail: zdy@hospital.cqmu.edu.cn (DYZ); Tel: +86-138-83517399; E-mail: u806806@cqmu.edu.cn (GHW)

References

[1] Liu Y. Renal fibrosis: new insights into the pathogenesis and therapeutics. Kidney Int 2006; 69: 213-217.

[2] Djudjaj S and Boor P. Cellular and molecular mechanisms of kidney fibrosis. Mol Aspects Med 2019; 65: 16-36.

[3] Nie J and Hou FF. Role of reactive oxygen species in the renal fibrosis. Chin Med J (Engl) 2012; 125: 2598-2602.

[4] Liu B, Ding FX, Liu Y, Xiong G, Lin T, He DW, Zhang YY, Zhang DY and Wei GH. Human umbilical cord-derived mesenchymal stem cells conditioned medium attenuate interstitial fibrosis and stimulate the repair of tubular epithelial cells in an irreversible model of unilateral ureteral obstruction. Nephrology (Carlton) 2018; 23: 728-736.

[5] Zhu XY, Lerman A and Lerman LO. Concise review: mesenchymal stem cell treatment for ischemic kidney disease. Stem Cells 2013; 31: 1731-1736.

[6] Cheng K, Rai P, Plagov A, Lan X, Kumar D, Salhan D, Rehman S, Malhotra A, Bhargava K, Palestro CJ, Gupta S and Singhal PC. Transplantation of bone marrow-derived MSCs improves cisplatinum-induced renal injury through paracrine mechanisms. Exp Mol Pathol 2013; 94: 466-473.

[7] Lai RC, Arslan F, Lee MM, Sze NS, Choo A, Chen TS, Salto-Tellez M, Timmers L, Lee CN, El Oakley RM, Pasterkamp G, de Kleijn DP and Lim SK. Exosome secreted by MSC reduces myocardial ischemia/reperfusion injury. Stem Cell Res 2010; 4: 214-222.

[8] Valadi H, Ekström K, Bossios A, Sjöstrand M, Lee JJ and Lötvall JO. Exosome-mediated transfer of mRNAs and microRNAs is a novel mechanism of genetic exchange between cells. Nat Cell Biol 2007; 9: 654-659.
[9] Zhang S, Chuah SJ, Lai RC, Hui J, Lim SK and Toh WS. MSC exosomes mediate cartilage repair by enhancing proliferation, attenuating apoptosis and modulating immune reactivity. Biomaterials 2018; 156: 16-27.
[10] Xiao C, Wang K, Xu Y, Hu H, Zhang N, Wang Y, Zhong Z, Zhao J, Li Q, Zhu D, Ke C, Zhong S, Wu X, Yu H, Zhu W, Chen J, Zhang J, Wang J and Hu X. Transplanted mesenchymal stem cells reduce autophagic flux in infarcted hearts via the exosomal transfer of mir-125b. Circ Res 2018; 123: 564-578.
[11] Sun L, Li D, Song K, Wei J, Yao S, Li Z, Su X, Ju X, Chao L, Deng X, Kong B and Li L. Exosomes derived from human umbilical cord mesenchymal stem cells protect against cisplatin-induced ovarian granulosa cell stress and apoptosis in vitro. Sci Rep 2017; 7: 2552.
[12] Liu B, Ding F, Hu D, Zhou Y, Long C, Shen L, Zhang Y, Zhang D and Wei G. Human umbilical cord mesenchymal stem cell conditioned medium attenuates renal fibrosis by reducing inflammation and epithelial-to-mesenchymal transition via the TLR4/NF-κB signaling pathway in vivo and in vitro. Stem Cell Res Ther 2018; 9: 7.
[13] Lee YH, Cheng FY, Chiu HW, Tsai JC, Fang CY, Chen CW and Wang YJ. Cytotoxicity, oxidative stress, apoptosis and the autophagic effects of silver nanoparticles in mouse embryonic fibroblasts. Biomaterials 2014; 35: 4706-4715.
[14] Cheng X, Zheng X, Song Y, Qu L, Tang J, Meng L and Wang Y. Apocynin attenuates renal fibrosis via inhibition of NOXs-ROS-ERK-myofibroblast accumulation in UUO rats. Free Radic Res 2016; 50: 840-852.
[15] Cheng H, Bo Y, Shen W, Tan J, Jia Z, Xu C and Li F. Leonurine ameliorates kidney fibrosis via suppressing TGF-β and NF-κB signaling pathway in UUO mice. Int Immunopharmacol 2015; 25: 406-415.
[16] Ding DC, Chang YH, Shyu WC and Lin SZ. Human umbilical cord mesenchymal stem cells: a new era for stem cell therapy. Cell Transplant 2015; 24: 339-347.
[17] Squillaro T, Peluso G and Galderisi U. Clinical trials with mesenchymal stem cells: an update. Cell Transplant 2016; 25: 829-848.
[18] Nakamura Y, Miyaki S, Ishitobi H, Matsuyama S, Nakasa T, Kamei N, Akimoto T, Higashi Y and Ochi M. Mesenchymal-stem-cell-derived exosomes accelerate skeletal muscle regeneration. FEBS Lett 2015; 589: 1257-1265.
[19] Baglio SR, Rooijers K, Koppers-Lalic D, Verweij FJ, Pérez Lanzón M, Zini N, Naaijkens B, Perut F, Niessen HW, Baldini N and Pegtel DM. Human bone marrow- and adipose-mesenchymal stem cells secrete exosomes enriched in distinctive miRNA and tRNA species. Stem Cell Res Ther 2015; 6: 127.
[20] Zhang J, Li S, Li L, Li M, Guo C, Yao J and Mi S. Exosome and exosomal microRNA: trafficking, sorting, and function. Genomics Proteomics Bioinformatics 2015; 13: 17-24.
[21] Lai RC, Yeo RW and Lim SK. Mesenchymal stem cell exosomes. Semin Cell Dev Biol 2015; 40: 82-88.
[22] Otunctemur A, Ozbek E, Cakir SS, Polat EC, Dursun M, Cekmen M, Somay A and Ozbay N. Pomegranate extract attenuates unilateral ureteral obstruction-induced renal damage by reducing oxidative stress. Urol Ann 2015; 7: 166-171.
[23] Yuan J, Shen Y, Yang X, Xie Y, Lin X, Zeng W, Zhao Y, Tian M and Zha Y. Thymosin β4 alleviates renal fibrosis and tubular cell apoptosis through TGF-β pathway inhibition in UUO rat models. BMC Nephrol 2017; 18: 314.
[24] Bonora M, Wieckowsk MR, Chinopoulos C, Kepp O, Kroemer G, Galluzzi L and Pinton P. Molecular mechanisms of cell death: central implication of ATP synthase in mitochondrial permeability transition. Oncogene 2015; 34: 1608.
[25] Basile DP, Donohoe D, Roethe K and Osborn JL. Renal ischemic injury results in permanent damage to peritubular capillaries and influences long-term function. Am J Physiol Renal Physiol 2001; 281: F887-899.
[26] Noiri E, Nakao A, Uchida K, Tsukahara H, Ohno M, Fujita T, Brodsky S and Goligorsky MS. Oxidative and nitrosative stress in acute renal ischemia. Am J Physiol Renal Physiol 2001; 281: F948-957.
[27] Palipoch S, Punsawad C, Koomhin P and Suwannalert P. Hepatoprotective effect of curcumin and alpha-tocopherol against cisplatin-induced oxidative stress. BMC Complement Altern Med 2014; 14: 111.
[28] Ratliff BB, Abdulmahdi W, Pawar R and Wolin MS. Oxidant mechanisms in renal injury and disease. Antioxid Redox Signal 2016; 25: 119-146.
[29] Ayala A, Muñoz MF and Argüelles S. Lipid peroxidation: production, metabolism, and signaling mechanisms of malondialdehyde and 4-hydroxy-2-nonenal. Oxid Med Cell Longev 2014; 2014: 360438.
[30] Javad-Mousavi SA, Hemmati AA, Mehrzadi S, Hosseinzadeh A, Houshmand G, Rashidi Nooshabadi MR, Mehrabani M and Goudarzi M. Protective effect of Berberis vulgaris fruit

extract against Paraquat-induced pulmonary fibrosis in rats. Biomed Pharmacother 2016; 81: 329-336.

[31] Xie X, Zhao Y, Ma CY, Xu XM, Zhang YQ, Wang CG, Jin J, Shen X, Gao JL, Li N, Sun ZJ and Dong DL. Dimethyl fumarate induces necroptosis in colon cancer cells through GSH depletion/ROS increase/MAPKs activation pathway. Br J Pharmacol 2015; 172: 3929-3943.

[32] Sun Y, Liu WZ, Liu T, Feng X, Yang N and Zhou HF. Signaling pathway of MAPK/ERK in cell proliferation, differentiation, migration, senescence and apoptosis. J Recept Signal Transduct Res 2015; 35: 600-604.

[33] Li J, Wang F, Xia Y, Dai W, Chen K, Li S, Liu T, Zheng Y, Wang J, Lu W, Zhou Y, Yin Q, Lu J, Zhou Y and Guo C. Astaxanthin pretreatment attenuates hepatic ischemia reperfusion-induced apoptosis and autophagy via the ROS/MAPK pathway in mice. Mar Drugs 2015; 13: 3368-3387.

[34] Zhang B, Wu T, Wang Z, Zhang Y, Wang J, Yang B, Zhao Y, Rao Z and Gao J. p38MAPK activation mediates tumor necrosis factor-α-induced apoptosis in glioma cells. Mol Med Rep 2015; 11: 3101-3107.